Lysosomal lipid accumulation from oxidized low density lipoprotein is correlated with hypertrophy of the Golgi apparatus and trans-Golgi network

W. Gray Jerome[1,*] Carol Cash,[*] Richard Webber,[†] Roger Horton,[†] Patricia G. Yancey[*]

Departments of Pathology[*] and Dentistry,[†] Wake Forest University School of Medicine, Winston-Salem, NC 27157-1092

Abstract **Lipid accumulation within macrophages is a major sequelae of atherosclerosis. Much of this lipid accumulation occurs within large, swollen lysosomes. We analyzed lipid accumulation in cultured macrophages using oxidized or acetylated low density lipoprotein (LDL) as the loading agent. Pigeon macrophages incubated for 48 h with mildly oxidized pigeon LDL (TBARS = 5–10 nmol/mg protein) showed significant increases in cellular cholesterol compared with untreated controls. Forty-eight percent of the increased cholesterol occurred as unesterified cholesterol. Treated cells had lipid-swollen lysosomes similar to those of atherosclerotic foam cells. The increase in lysosomal lipid was accompanied (correlation coefficient of 0.96) by increases in acid phosphatase staining cisternae of the Golgi and trans-Golgi network (TGN). THP-1 macrophages incubated with oxidized LDL showed similar lysosomal loading and Golgi/TGN hypertrophy. In contrast, macrophages incubated with acetylated LDL accumulated significant amounts of cholesterol but the increase occurred as cholesteryl ester (81% in pigeons) within cytoplasmic droplets and there was no associated increase in acid phosphatase-containing cisternae of Golgi or TGN. The correlation in both pigeon and THP-1 macrophages of oxidized LDL-induced lysosomal lipid accumulation and Golgi hypertrophy suggests a linkage of these two phenomena. This implicates intracellular membrane trafficking as a possible defect in foam cells of the atherosclerotic lesion.—**Jerome, W. G., C. Cash, R. Webber, R. Horton, and P. G. Yancey. **Lysosomal lipid accumulation from oxidizied low density lipoprotein is correlated with hypertrophy of the Golgi apparatus and trans-Golgi network. *J. Lipid Res.* 1998.** 39: **1362–1371.**

Supplementary key words atherosclerosis • macrophage • THP-1 • pigeon • acetylated LDL

An early event in atherosclerosis is the engorgement of macrophages with lipid. At specific stages of atherogenesis in both humans and animal models, this lipid is found within large, swollen lysosomes (1–4). This lysosomal lipid accumulation is a little-studied feature of lesion development. However, several lines of evidence suggest that this lysosomal sequestration may be an important component of the disease. Foremost is the ubiquitous nature of lysosomal lipid accumulation as a disease sequelae. In addition, the timing and spatial location of lysosomal accumulation coincide with the stimulation of smooth muscle proliferation and migration into the intima (5). Moreover, lysosomal cholesteryl esterase activity has been correlated with extent and severity of the disease (6) and regression studies suggest that lysosomally sequestered cholesterol is less available for efflux (7).

Low density lipoprotein (LDL) is the major contributor of cholesterol to atherosclerotic foam cells. Receptor-mediated uptake of normal LDL in cultured macrophages initially delivers cholesterol to lysosomes for processing (8, 9). In the lysosomes, acid lipases hydrolyze cholesteryl esters. The resulting unesterified cholesterol readily leaves the lysosome (10) where it can be incorporated into membranes or stored in cytoplasmic droplets by reesterification of the cholesterol. It is not clear why, in atherosclerotic foam cells, the normal clearance pattern is not operational or is insufficient to clear the internalized lipid from lysosomes.

It is known that specific alterations in lipoproteins that make them more atherogenic can also profoundly influence their metabolism (10–12). This can be mediated at the level of uptake (10) but alterations have other effects as well and can alter their rate of trafficking and metabolism (13, 14). Oxidation is a lipoprotein modification that has been linked to atherosclerosis (15). Oxidation clearly increases LDL uptake (15). However, subsequent cholesterol processing is also affected. These effects include the buildup of unesterified cholesterol within foam cell lysosomes (16, 17).

Abbreviations: ACAT, acyl-CoA:cholesterol acyltransferase; BSA, bovine serum albumin; DMEM, Dulbecco's modified Eagle's medium; FBS, fetal bovine serum; MEM, minimum essential medium; PPACK, d-phyenylalanyl-l-propyl-l-arginine chloromethylketone; TACT, tuned aperture computed tomography; TBARS, thiobarbituric acid-reactive substances; TLC, thin layer chromatography; TGN, the trans-Golgi network; WC, White Carneau.

[1]To whom correspondence should be addressed.

In this study we combine morphological and biochemical techniques to show that formation of unesterified cholesterol-rich lysosomes is accompanied by extensive hypertrophy of elements of the secretory pathway, specifically Golgi and trans-Golgi network. These elements contain hydrolase activity and the hypertrophy is quantitatively related to the degree of lysosomal engorgement. This suggests that, in part, the lysosomal cholesterol accumulate may be the result of a defect in intracellular traffic mechanisms.

MATERIALS AND METHODS

Materials

Eagle's minimum essential medium (MEM), Dulbecco's modified Eagle's media (DMEM), RPMI, Eagle's vitamins, l-glutamine, penicillin, and streptomycin were obtained from Mediatech, Washington, DC. Fetal bovine serum (FBS) and chick serum were from ICN/Flow, Costa Mesa, CA. Serum was heat-inactivated before use by incubation at 56°C for 1 h. Aprotinin and phenylmethylsulfonylfluoride were purchased from Boehringer Mannheim Corp., Indianapolis, IN. d-Phenylalanyl-l-propyl-l-arginine chloromethyl ketone (PPACK) was purchased from Calbiochem Corp., San Diego, CA. Stigmasterol, cholesterol, and thin-layer chromatography (TLC) standards were purchased from Steraloids, Wilton, NH. LK6D Silica gel 60 thin-layer chromatography plates were from Whatman Ltd. Clifton, NJ. All tissue-culture plasticware was obtained from Falcon, Lincoln Park, NJ. Bovine serum albumin (BSA; fatty acid-free from fraction V) and EDTA were purchased from Sigma Chemical Company, St. Louis, MO. All chemical solvents and other chemical reagents were purchased from Fisher Scientific, Pittsburgh, PA.

Lipoprotein isolation

Pigeon low density lipoprotein (LDL) was isolated from blood obtained from male random bred WC pigeons. The pigeons are from a closed colony maintained at Wake Forest University School of Medicine. All animal use and veterinary care was under the supervision of the Institutional Animal Use and Care Committee. Male birds were chosen to minimize triglyceride levels that are elevated in female plasma during egg-laying periods. Blood was collected by venous puncture into tubes containing aprotinin (25 kallikrein inhibitory units/ml), PPACK (1 μm), and phenylmethylsulfonylfluoride (0.5 mm). Pigeon LDL (d 1.006–1.063 g/ml) was isolated from pooled plasma by density gradient ultracentrifugation using KBr to adjust plasma density (18). After dialysis with NaCl, the lipoproteins were filter-sterilized (0.45 μm acrodisc filter) and stored at 4°C until used. All lipoproteins were used within 4 weeks of isolation.

Pigeon LDL was acetylated using the method of Basu et al. (19). Pigeon LDL is less oxidizable than human LDL and so for mild oxidation it was dialyzed against 10 μm $CuSO_4$ in 0.9% NaCl for 12 h at 20°C. The extent of oxidation was estimated as thiobarbituric acid reactive substances (TBARS) measured at 535 nm using the method described by Buege and Aust (20). To control for effects of differing oxidation levels, we used only LDL mildly oxidized within a narrow range (TBARS = 5–10 nmol/mg LDL protein). The migration of the oxidized LDL (ox-LDL) preparations on 0.5% agarose gel did not vary substantially from that of normal pigeon LDL while acetylated LDL (ac-LDL) showed substantial migration from the origin. Normal and altered lipoproteins were analyzed for protein content using the method of Lowry et al. (21). Cholesterol content was determined by GLC (22). The mild oxidation of LDL used in these studies did not reduce the cholesterol content by more than 1% in any preparation, and greater than 80% of the cholesteryl ester in the particles remained unmodified when analyzed by thin-layer chromatography.

The lack of changes in cell number with lipoprotein incubation were confirmed by comparing protein per dish between treated and untreated cultures and by counting the number of cells in 25 arbitrarily selected, non-adjacent microscope fields at 200 × magnification using an inverted microscope.

Cell isolation and culture

Pigeon monocytes were isolated by differential centrifugation of citrated whole blood acquired by venipuncture of random-bred White Carneau pigeons, as routinely done in our lab (23). Monocytes were washed and plated at 2.0–4.0 × 10^5 cells/ml in 35-mm culture dishes. Cultures were maintained at 37°C in a 5% CO_2, humidified incubator for 24 h in MEM containing 10% (V/V) heat-inactivated chicken serum and supplemented with vitamins, 200 mm l-glutamine, 10 mm HEPES, 100 IU/ml each of penicillin and streptomycin. After 24 h, the cultures were washed to remove non-adherent cells and the culture medium was replaced with medium containing fetal bovine serum (FBS) instead of chicken serum. The use of fetal bovine serum minimizes lipid uptake, as pigeon macrophages are relatively incapable of acquiring cholesterol from this source (22). On day 5, culture medium was exchanged with culture medium in which serum was replaced with essentially fatty acid-free BSA, to reduce cellular triglyceride, and maintained in this medium for 36 hours.

THP-1 cells, obtained from ATCC of Rockville, MD, were maintained in RPMI-1640 medium supplemented with 10% FBS and 0.0009% mercaptoethanol. For the experiments, the cells were plated onto 35-mm wells at a density of 1.5 × 10^6 cells, and incubated for 3 days in RPMI-1640 containing 10% FBS and 100 ng phorbol ester/ml of medium. Experiments were initiated 3 days after plating.

Cellular cholesterol loading and estimation of cellular lipid mass

To load cells with cholesterol, monocytes were incubated in medium containing 1% FBS and the indicated concentration of lipoprotein. Cells were exposed to the lipoprotein for 48 h. Some cultures were analyzed immediately, but in most cultures the lipoprotein-containing medium was replaced with medium containing only 1% FBS for an additional 24 h to allow lysosomal hydrolysis and cholesterol clearance to continue. Control cells were maintained in culture with 1% FBS but no lipoprotein.

Total and free cholesterol was assayed from aliquots of isopropanol extracts (24) and determined by GLC (22) after isolation using the procedure of Ishikawa et al. (25) with stigmasterol as an internal standard. Esterified cholesterol mass was estimated as the difference between total and free. Cellular protein was assayed using the Lowry procedure (21) using bovine serum albumin for a standard.

Electron microscopy

After lipid loading, cells for thin section ultrastructural examination were washed in cacodylate buffer and fixed in 2.5% glutaraldehyde. Lysosomes and related organelles were localized by the presence of acid phosphatase. To demonstrate acid phosphatase, samples were processed using a modification of the Gomori (26) lead precipitation method (1). The reaction control was incubated in the identical medium but without the beta-glycerophosphate substrate. After cytochemical incubation, cells were postfixed in 1% osmium tetroxide, en bloc stained with uranyl acetate, dehydrated, and embedded in epoxy resin.

The volume of the cell occupied by lysosomes, cytoplasmic

droplets, and acid phosphatase-positive tubules was estimated using point counting stereology techniques (27). Acid phosphatase containing tubules were only counted when their lumen measured less than 100 nm. In this way we avoided counting tubular lysosomes and other endocytic organelles. For pigeon macrophages, 10 randomly chosen areas from each of 10 arbitrarily selected sections were quantified at a magnification of 38,000×. Sections and areas were chosen such that no cell was sampled more than once. The number of cells in any given area varied, but the total cellular area sampled averaged 2,700 μm^2 for each condition. The mean and standard error were calculated for each group of 10 fields (n = 10). Comparison of the volume of cell occupied by TGN for each condition was done with Tukey's multiple comparison test after analysis of variance. In all cases, percentage data was transformed using the arcsin transform prior to analysis.

3-D quantitative analysis using TACT

Stereology describes a population rather than individual cells. Thus, additional studies using Intermediate voltage electron microscopy of thick sections were undertaken to correlate increases in acid phosphatase-containing tubules with lysosomal engorgement in individual cells. As the lipid-engorged lysosomes were smaller (largest lysosomes = 2.6 μm) than the section thickness (3.0 μm), the volume of individual lysosomes and the trans-Golgi network (TGN) could be ascertained. Quantitation of thick sections used Tuned Aperture Computed Tomography (TACT). TACT is a general series of algorithms for 3-D imaging of thick material (28, 29). We have adapted these algorithms for use with thick section-IVEM microscopy. TACT is related to Computed Axial Tomography (CAT scan). Like CAT, the TACT input is a series of projection images through a 3-D volume taken at different angles. Unlike CAT, for TACT only a few projections are required; this simplifies the computations. Although not as high resolution a procedure as CAT, TACT is a simpler procedure and is easily quantified. The computations produce a series of images representing parallel slices through the volume, analogous to the thin focal planes of confocal microscopy. The volume of individual organelles is computed by measuring the area in each computer-reconstructed slice, multiplying by the slice thickness to obtain a volume, and then summing all the volumes. This allows analysis of single cells and single organelles within a cell.

One strength of the TACT procedure is that it allows one to set the total angular spread of the series and the individual tilt increments to match the accuracy needed. Thus, extra manual and computational work can be avoided. Under test conditions, using similar parameters and sample thickness, TACT reconstructions displayed images of 20 nm colloidal gold particles with less than 0.1% distortion along the X and Y axes. Distortion along the Z axis was only 4.5% (the average diameter of 20 nm spheres appeared as 20.9 nm along the Z axis). The Z axis resolution is determined by the angular spread of the tilts. To increase efficiency of data collection, we set our computed slice thickness to 50 nm. Thus the accuracy along the Z axis and the corresponding accuracy of our measurements are set by the slice thickness that is larger than the inherent Z resolution of the conditions. The extreme differences seen between the cells chosen allowed us to use this less stringent slice thickness.

The lysosomal lipid volume and volume of acid phosphatase-positive Golgi-TGN were analyzed for four pigeon monocytes with differing levels of lipid accumulation. Image magnification was 50,000×. Forty-one images were taken of each cell. These images encompassed an angular spread between +40 and −40 degrees of tilt at 2 degree increments. A series of continuous slices of 50 nm thickness along the Z axis was computed and the volume of lysosome and Golgi-TGN was determined from these slices. As both lysosomal lipid and the Golgi-TGN are principally in more central regions of the cell and our sections were chosen to include these areas, the analysis involves most of the lysosomal lipid and Golgi-TGN within each cell analyzed. The correlation of lysosomal volume with tubular volume was determined using simple linear regression analysis.

RESULTS

Treatment of pigeon macrophages with oxidized LDL but not acetylated LDL leads to increases in cellular unesterified cholesterol

When pigeon monocyte-derived macrophages were incubated for 48 h with 100 μg/ml copper-oxidized LDL and then allowed a 24-h clearance period without ox-LDL, there was an increase in both esterified and unesterified cholesterol compared with the 0-h control. **Figure 1** shows the results of a representative experiment. Prior to incubation, cells had only 24 μg free cholesterol/mg cell protein and the esterified cholesterol content of these cells was negligible. After 48 h, free cholesterol had increased to 87 μg/mg cell protein and esterified cholesterol increased to 94 μg/mg cell protein. The increase in unesterified cholesterol represented a more than 3.5-fold augmentation over the baseline level. In contrast, when pigeon macrophages were incubated under identical conditions with 100 μg/ml ac-LDL there was only a minor 60% increase in unesterified cholesterol (Fig. 1). The difference in free cholesterol levels was not due to a failure to internalize ac-LDL, as the ac-LDL-treated cells accumulated similar total cholesterol amounts. However, in the ac-LDL-treated cells, the accumulation occurred almost

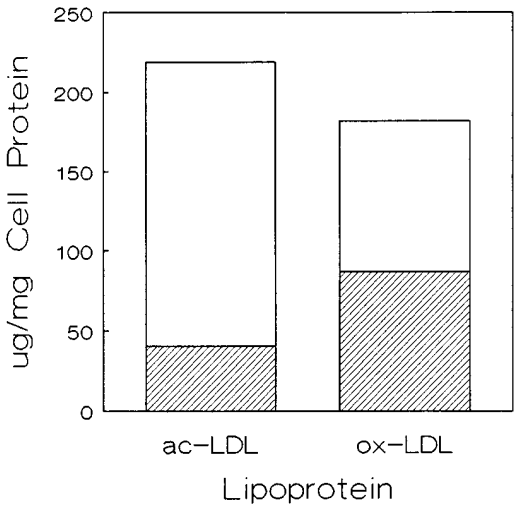

Fig. 1. Comparison of unesterified (hatched area of bar) and esterified cholesterol (open area of bar) accumulation in pigeon macrophages incubated with ac-LDL or ox-LDL. Macrophages were incubated with lipoprotein for 48 h followed by a 24-h equilibration phase without lipoprotein. Both ac-LDL and ox-LDL produced significant ($P < 0.05$) total cholesterol accumulation. Ac-LDL produced increases predominantly in esterified cholesterol. In contrast, ox-LDL led to accumulation of both free and esterified cholesterol.

entirely as esterified cholesterol. Cell numbers and total protein per dish were similar for both acetylated LDL and oxidized LDL-treated cells and did not change appreciably during the experiments. There was no evidence of cytotoxicity with our oxidized LDL preparations. There was no stored lipid evident in untreated cells.

Incubation of pigeon macrophages with ox-LDL but not acetylated LDL produced large, lipid-swollen lysosomes

Ultrastructural observation showed that cells incubated for 48 h with ox-LDL followed by a 24-h clearance period accumulated lipid within large lysosomes. A typical cell can be seen in **Fig. 2A**. The dark acid phosphatase reaction product highlights the lysosomal character of the lipid deposits. Stereologic quantitation of the cells revealed that 46% of the cell volume was occupied by lipid, with 65% of that lipid within lysosomes (**Fig. 3**). The remaining 35% occurred as free cytoplasmic droplets, presumably reesterified cholesteryl ester. Stored lipid in acetylated LDL-treated cells also occupied approximately 42% of the cell volume. However, with acetylated LDL treatment, cells accumulated this lipid almost entirely within cytoplasmic droplets that lacked both acid phosphatase activity and a limiting bilayer membrane (Fig. 2B). The predominant (81%) form of cholesterol stored in ac-LDL-treated cells was cholesteryl ester (Fig. 3). The differences in distribution were evident despite similarities in total cholesterol levels for the two treatments.

Ox-LDL but not ac-LDL-induced hypertrophy of tubular organelles related to the Golgi apparatus and trans-Golgi network

As demonstrated in Fig. 2 and **Fig. 4**, accompanying lysosomal cholesterol accumulation from ox-LDL there was a noticeable increase in acid phosphatase-containing tubules within the cells compared with untreated cells. The location and acid phosphatase staining of the cisternae confirms that these cisternae were elements of the trans-most regions of the Golgi and the TGN. The TGN was more pleiomorphic than the trans-Golgi cisternae but both occurred in close proximity and we did not distinguish between the two in our quantitation. Quantitation was based on acid phosphatase staining. However, to be sure that there was a true hypertrophy of the Golgi and TGN rather than merely a shift in staining pattern, we quantified the total Golgi/TGN volume for one group of cells treated with ox-LDL and one ac-LDL-treated group. There was no significant ($P < 0.05$) difference in unstained elements between the two groups ($0.32 \pm 0.04\%$ of cell volume versus $0.28 \pm 0.04\%$ of cell volume, respectively). Thus, the elevation in acid phosphatase stained elements represents an increase in cisternal elements.

The increases in acid phosphatase-positive tubules were apparent in thin sections through the cells. However, the nature and extent of the tubules was best seen in thick sections viewed by intermediate voltage electron microscopy (**Fig. 5**). Stereologic quantitation of the volume of the tubules using thin sections confirmed an increase in tubules

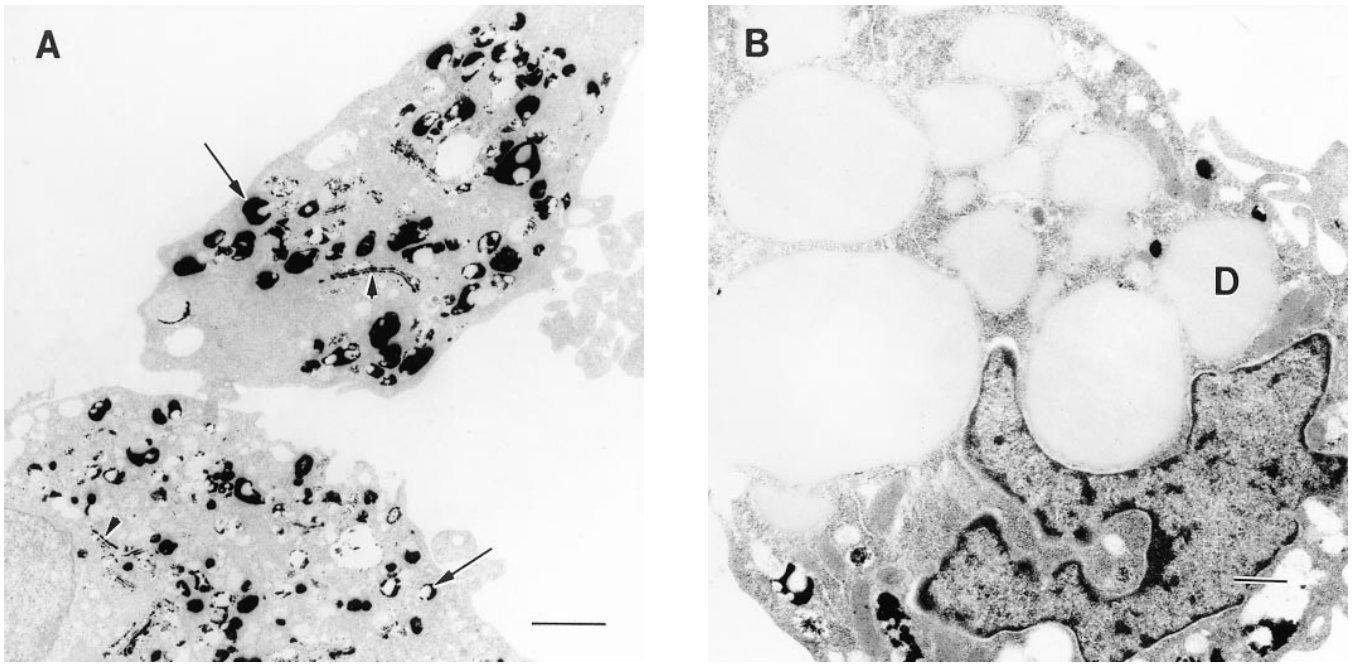

Fig. 2. Electron micrographs of cellular lipid accumulation in pigeon macrophages incubated for 48 h with ox-LDL or ac-LDL followed by a 24-h equilibration phase. The cells in these and all other electron micrographs are unstained except for the acid phosphatase reaction and the osmium postfixation. A: Cells incubated with ox-LDL had large, lipid-swollen lysosomes. The lysosomes were highlighted by the presence of dark acid-phosphatase reaction product (arrow). In addition, the cells contained prominent acid phosphatase-stained cisternae of the Golgi apparatus and trans-Golgi network. Magnification = 9,900×, bar = 1 μm. B: Cell incubated with ac-LDL showing lipid accumulation primarily as non-stained cytoplasmic droplets (D). Magnification = 13,300×, bar = 0.5 μm.

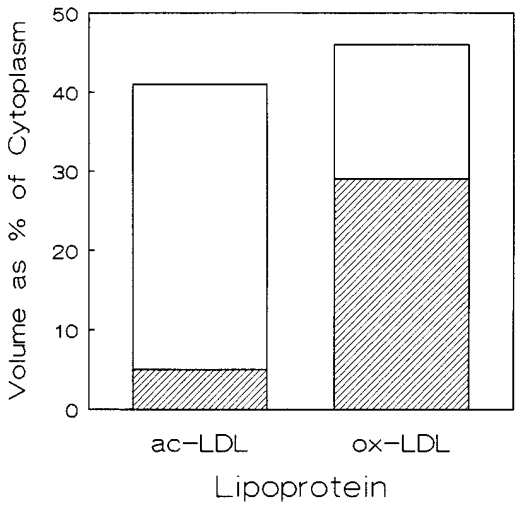

Fig. 3. Quantitation of lysosomal (hatched area of bar) and cytoplasmic (open area of bar) lipid accumulation in pigeon macrophages incubated with ac-LDL or ox-LDL. Macrophages were incubated with lipoprotein for 48 h followed by a 24-h equilibration phase without lipoprotein. Both ac-LDL and ox-LDL produced significant ($P < 0.05$) lipid accumulation (occupying more than 40% of the cytoplasmic volume) compared to cells prior to treatment where no cellular lipid stores were detected. With ac-LDL this increase was primarily as cytoplasmic lipid droplets while ox-LDL produced increases in both cytoplasmic droplets and lysosomes.

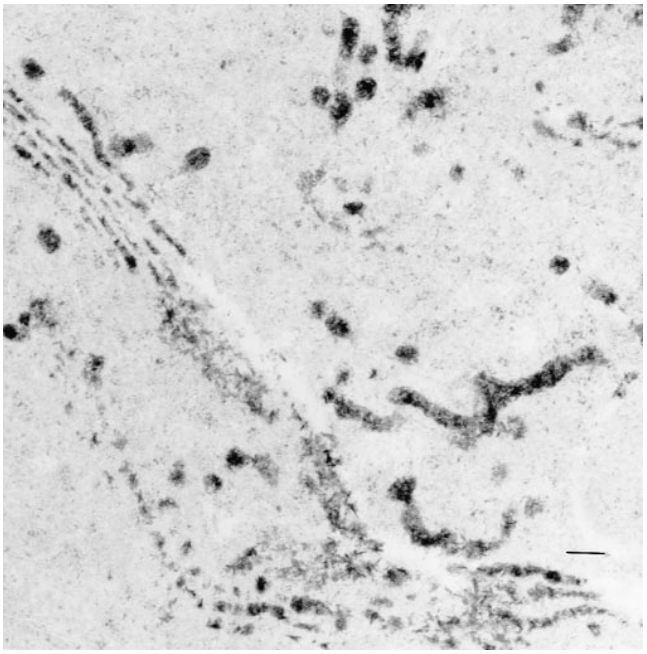

Fig. 4. Electron micrograph of stained cisternae in a pigeon macrophage incubated with ox-LDL for 48 h followed by 24 h equilibration without lipoprotein. Staining can be seen in both the parallel cisternae of the trans area of the Golgi apparatus as well as in the pleiomorphic tubules and vesicles of the trans-Golgi network. Magnification = 69,300×, bar = 0.1 μm.

after 48-h loading with ox-LDL (**Fig. 6**). This increase was absent when ac-LDL was the loading vehicle. With normal culture conditions, acid phosphatase-containing tubules occupied 0.3% of the pigeon macrophage cytoplasmic volume. There was no significant change in this parameter when cells were incubated for 48 h with ac-LDL and then allowed a 24-h clearance period. In contrast, when pigeon macrophages were incubated for 48 h with ox-LDL and then cleared for 24 h, there was a significant ($P < 0.05$) 5-fold increase in acid phosphatase-containing tubular organelles. IVEM images also revealed that tubules changed their appearance with ox-LDL treatment, becoming more pleiomorphic and resembling the TGN more than elements of the Golgi apparatus. A similar hypertrophy of the TGN was observed corresponding to lysosomal lipid accumulation when THP-1 macrophages were treated with human ox-LDL (data not shown). Thus, lysosomal lipid accumulation was accompanied by an increase in the number and length of acid hydrolase containing tubules of the Golgi-TGN networks.

There was a strong statistical correlation between the volume of lysosomal lipid and the volume of acid phosphatase-positive tubules

The stereologic quantitation above demonstrated that the population of cells incubated with ox-LDL showed both an increase in lysosomal lipid volume and volume of TGN. We next asked whether the same cells showing increased lysosomal lipid also showed an increase in the extent of stained TGN. Determination of the volume of lipid-filled lysosomes or acid phosphatase-positive tubules in single cells cannot be done using thin-section stereology techniques. Instead, the volumes of these two compartments were estimated in four ox-LDL-treated cells with different levels of lipid accumulation using TACT for the reconstructions. As shown in **Fig. 7**, cells with the greatest amount of lysosomal lipid also showed the largest degree of tubular hypertrophy. Correlation analysis of tubule volume and lysosomal volume showed a highly significant coefficient of 0.96, suggesting that the two phenomena were related.

Lysosomal lipid accumulation in response to pigeon ox-LDL was not specific for pigeon monocyte-derived macrophages

When PMA-activated THP-1 macrophages were incubated with pigeon ox-LDL for 72 h followed by a 24-h clearance period, the cells accumulated lipid within lipid-swollen lysosomes similar to those seen with pigeon macrophages (**Fig. 8**). Lipid occupied 21% of the cell volume with 72% of that being as lysosomal lipid (**Fig. 9**). As with pigeon macrophages, acid phosphatase-positive tubules were more prevalent in ox-LDL-treated THP-1 cells (**Fig. 10**). Acetylated LDL, on the other hand, produced primarily cytoplasmic droplets, lacking acid phosphatase activity (Fig. 9) and no increase in tubules was apparent (Fig. 10).

DISCUSSION

The exact in vivo mechanisms of atherosclerotic foam cell formation are not known. We show here that incuba-

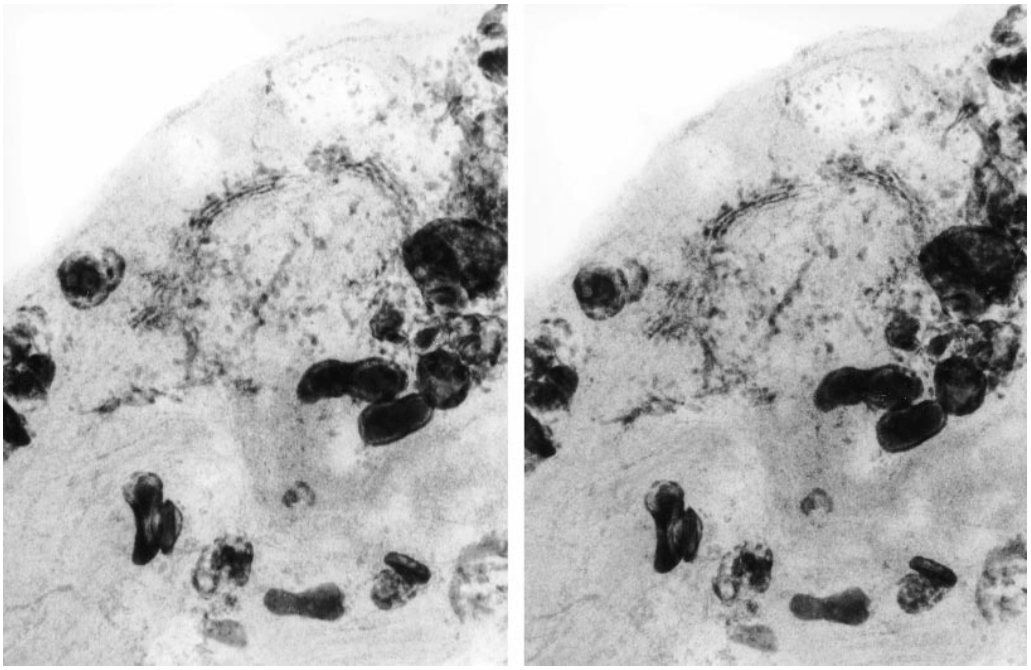

Fig. 5. Stereo pair micrographs of a pigeon macrophage incubated with ox-LDL for 48 h followed by 24 h equilibration without lipoprotein. This thick section view shows the 3-D arrangement and extent of the tubular hypertrophy occurring as a result of incubation of cells with ox-LDL. In addition, a number of large, spherical, lipid-filled lysosomes are also present, identified by the dark reacton product around the periphery of the central lipid core. Magnification = 24,300×.

tion of cultured macrophages from humans and pigeons with oxidized LDL produces a lysosomal lipid accumulation similar to that seen in atherosclerotic arteries. This is significant, as lipoprotein oxidation has been linked to atherosclerosis (15). Prior studies from other labs have also suggested that oxidation of LDL affects its cellular metabolism in ways that lead to lysosomal accumulation. Oxidation clearly increases LDL uptake (15) and appears to decrease lysosomal protein hydrolysis (30) and the ability of lipoprotein cholesterol to stimulate acyl-CoA:cholesterol acyltransferase (ACAT)-mediated reesterification

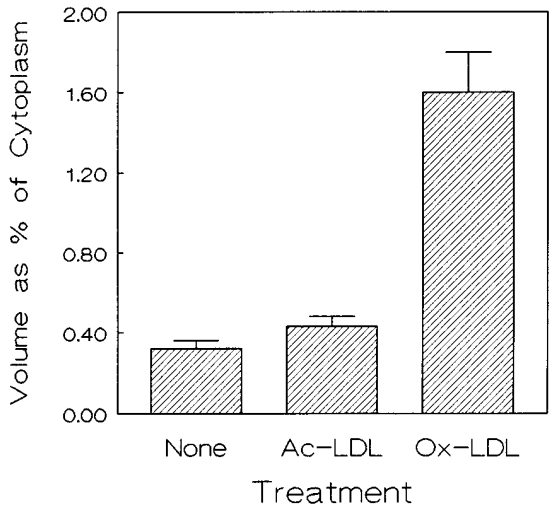

Fig. 6. Quantitation of the volume density (volume of cisternae as percent of total cytoplasmic volume of cell) of acid phosphatase-staining cisternae in pigeon macrophages incubated with ac-LDL or ox-LDL for 48 h followed by 24 h equilibration without lipoprotein. Bars represent the mean volume density (±SEM). ANOVA followed by Tukey's multiple comparison test indicated that incubation with ox-LDL but not ac-LDL produced a significant ($P < 0.05$) increase in the extent of stained cisternae.

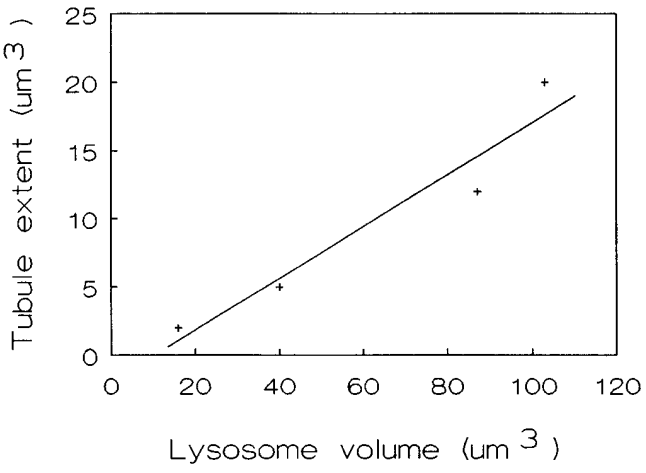

Fig. 7. Relationship of lysosomal volume and cisternal extent in four pigeon macrophages incubated for 48 h with ox-LDL followed by 24 h incubation without lipoprotein. Cells with greater lysosomal lipid accumulation also showed increased extent of acid phosphatase-positive cisternae of the Golgi and TGN. The correlation coefficient was 0.96.

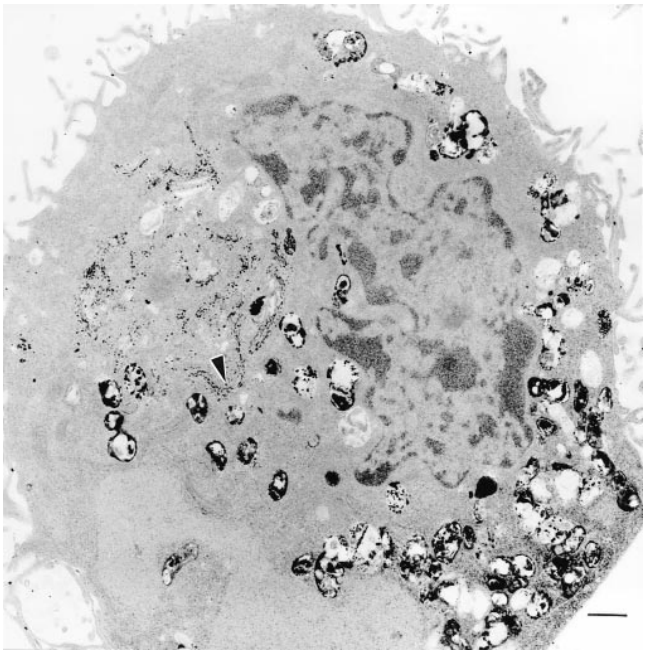

Fig. 8. Electron micrograph of cellular lipid accumulation in THP-1 macrophage incubated for 48 h with ox-LDL followed by a 24-h equilibration phase. Like pigeon cells, this cell has large, lipid-swollen lysosomes highlighted by the presence of dark acid-phosphatase reaction product. In addition, the cell contains prominent acid phosphatase-stained cisternae of the Golgi apparatus and trans-Golgi network (arrowhead). Magnification = 11,000×, bar = 0.5 μm.

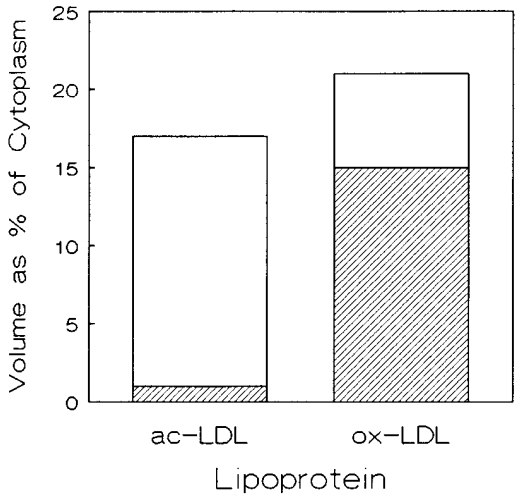

Fig. 9. Quantitation of lysosomal (hatched area of bar) and cytoplasmic (open area of bar) lipid accumulation in THP-1 macrophages incubated with ac-LDL or ox-LDL. Macrophages were incubated with lipoprotein for 72 h followed by a 24-h equilibration phase without lipoprotein. With both ac-LDL and ox-LDL lipid accumulation occupied between 15 and 20% of the cytoplasmic volume. With ac-LDL this increase was primarily as cytoplasmic lipid droplets while ox-LDL produced increases in both cytoplasmic droplets and lysosomes.

(31, 32). These findings suggest an accumulation of lipoprotein components within lysosomes. In studies of ox-LDL-treated J774 macrophages, Maor and Aviram (33) reported the accumulation of excess free cholesterol rather than ACAT-derived cholesteryl ester. Although the cell culture studies underscore the fact that ox-LDL can affect lysosomal function, they have generally reported cholesterol accumulation that is far less than that seen in atherosclerotic lesions. This may be because much of the cholesterol and cholesteryl ester in heavily oxidized LDL is modified (34–36). Indeed, ox-LDL that has been "re-enriched" with cholesterol can induce significantly increased macrophage cholesterol accumulation compared to ox-LDL lacking cholesterol re-enrichment (37). Our current study used a mildly oxidized LDL where most of the lipoprotein cholesterol was intact. Incubation with this mildly ox-LDL produced a more than 4-fold increase in total cholesterol in pigeon macrophages, equivalent to that seen with ac-LDL. Moreover, the accumulation of lipid in response to ox-LDL was not limited to pigeon macrophages, it was also seen with a human macrophage cell line (THP-1). The accumulation and metabolism of free cholesterol and cholesteryl esters from mildly oxidized LDL in different macrophage types is examined in more detail in a companion paper (38).

Additionally, this study shows that hypertrophy of the TGN accompanied the lysosomal lipid engorgement in pigeon macrophages incubated with pigeon ox-LDL. A similar hypertrophy was also observed in pigeon ox-LDL-treated THP-1 cells. While other studies have demonstrated that both ox-LDL and ac-LDL are internalized via scavenger receptors (39–41), our studies found that incubation of pigeon or THP-1 macrophages with ac-LDL did not lead to lysosomal lipid engorgement or TGN hypertrophy. The reasons why particles taken up by similar mechanisms produce such divergent results are unclear.

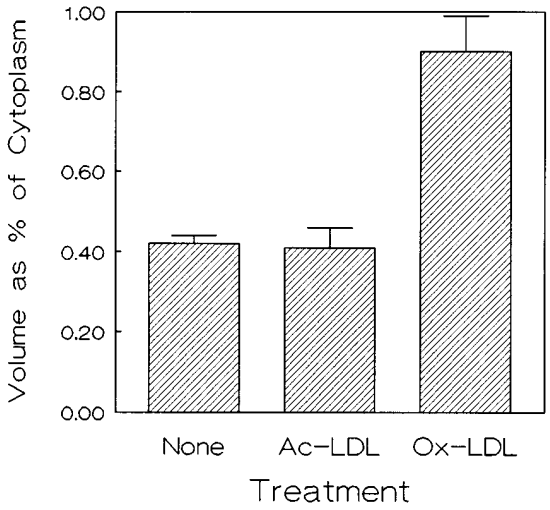

Fig. 10. Quantitation of the volume density of acid-phosphatase staining cisternae in THP-1 macrophages incubated with ac-LDL or ox-LDL for 72 h followed by 24 h equilibration without lipoprotein. Bars represent the mean volume density (±SEM). ANOVA followed by Tukey's multiple comparison test indicated that incubation with ox-LDL but not ac-LDL produced a significant ($P < 0.05$) increase in the extent of stained cisternae.

However, it is clear that lipid and protein oxidation products, such as those found in ox-LDL, can influence lysosomal metabolism of lipoprotein. For example, Lougheed, Zhang, and Steinbrecher (30) reported that the addition of oxidized fatty acids to LDL without any further oxidation was enough to make the protein component of LDL highly resistant to hydrolysis by cathepsins. In addition, studies by Maor, Mandel, and Aviram (42) suggest that 7-ketocholesterol in ox-LDL inhibits sphingomyelinase leading to a build-up of free cholesterol in lysosomes. Ox-LDL could, of course, work directly to stimulate increases in the Golgi membranes. However, a salient finding of this paper is that lysosomal loading and hypertrophy of the Golgi and TGN occur together and that hypertrophy is correlated with the degree of lysosomal lipid accumulation. This, certainly, does not prove that the two are directly related, but it does suggest that the two phenomena are in some way linked, particularly as loading cells to equivalent degrees of cholesterol with ac-LDL does not induce this hypertrophy. In addition, similar studies of the effects of oxidized LDL conducted with J774.A1 macrophages showed that lysosomal lipid accumulation was greatly reduced compared to that of THP-1 and pigeon macrophages. Most of the lipid accumulation occurred as cytoplasmic inclusions and the extent of Golgi/TGN membranes did not exceed 0.5% of the cell volume in these cells. Thus, even ox-LDL failed to induce membrane hypertrophy when given under conditions that did not promote lysosomal accumulation. This suggests that hypertrophy of the Golgi is not necessarily directly dependent upon ox-LDL, but rather could be a sequelae of the lysosomal lipid accumulation produced by ox-LDL. If this is true, then other perturbations that induce lysosomal lipid accumulation could also produce increases in Golgi membranes and, indeed, incubation of rabbit aortic smooth muscle cells with phospholipid–cholesteryl oleate–triolein dispersions produced significant lysosomal cholesterol accumulation (43). These rabbit studies also showed an increase in acid phosphatase-positive cisternae of the Golgi and TGN, specifically in cells containing lysosomal lipid.

The correlation of Golgi/TGN volume and lysosomal accumulation suggests an alteration in normal cellular trafficking. The trans elements of the Golgi and the TGN are dynamic structures involved in the sorting and trafficking of material for secretion or delivery to other membranous organelles, such as lysosomes (for review see (44, 45)). The TGN is particularly important for the correct packaging and delivery of hydrolases to the lysosomes. Communication between different elements of the Golgi and TGN occurs via transfer of vesicles or by formation of long tubules (46–48). The constant need to traffic material into and out of the Golgi produces a dynamic structure whose form is constantly changing and tubular extensions and vesicles, both manifestations of this exchange process, coexist in concert with each other. Whether tubules or vesicles predominate, may be, in part, dependent upon the environmental conditions (48, 49). Recent evidence shows dramatic accumulations of tubules when transport to distant destinations is blocked (46, 50, 51). Given this, the Golgi/TGN hypertrophy seen in our experiments suggests an alteration in membrane traffic when cells are treated with ox-LDL and may, in fact, reflect an inhibition of delivery of hydrolases to the lysosomes. Failure of hydrolase delivery would certainly lead to lysosomal accumulation of undigested material.

One possible means to influence trafficking, would be an increase in lysosomal membrane cholesterol such as one would expect with the increases in lysosomal free cholesterol noted in the current study. The cholesterol content of membranes can both directly and indirectly affect membrane function (52). Moreover, peroxidation of lipids has been shown to decrease membrane fluidity (53) and it is known that trafficking of vesicles and their contents can be influenced by the lipid component of membranes (54–56). One could speculate, therefore, that increased lysosomal membrane cholesterol or oxidation products might influence trafficking to and from the lysosomes. In this scheme, free cholesterol accumulation in lysosomes would lead to increased membrane cholesterol levels that would, in turn, cause defective trafficking of material. This trafficking failure could potentially lead to a failure of proper delivery of lysosomal hydrolases. In this scenario, continued uptake of lipoprotein without lysosomal hydrolases would lead to the accumulation of unhydrolyzed lipoprotein cholesteryl esters in the lysosomes. In a companion paper we demonstrate that, indeed, this is what occurs (38).

Although more data are clearly required to add credence to our speculation regarding abnormal delivery of hydrolase to lysosomes, it should be noted that hypertrophy of the TGN is a feature of Tangier disease (57). This disease is characterized by abnormal cholesterol processing and an accumulation of lipoprotein cholesterol within lysosomes. In Tangier patients there is also a dramatic increase in phospholipid synthesis. It has been hypothesized that the increases in TGN membrane in Tangier patients is a consequence of the increased phospholipid synthesis rather than a failure of trafficking between TGN and lysosomes (57). However, the two hypotheses are not necessarily mutually exclusive. In Niemann-Pick type C disease, another disorder characterized by lysosomal lipid accumulation, TGN and trans-Golgi membranes become enriched in cholesterol (58). Although the degree of hypertrophy seen in Tangier patients is not present in Niemann-Pick cells, the Golgi morphology is abnormal, again suggesting a tie-in between cholesterol traffic and increases in Golgi and TGN membranes. Furthermore, cellular accumulation of free cholesterol is known to stimulate phospholipid synthesis, presumably as a means of detoxifying the potentially harmful free cholesterol (59). Thus all of these phenomena (increased lysosomal cholesterol, increased membrane cholesterol, and increased membrane synthesis) appear interrelated. This suggests that lysosomal free cholesterol buildup potentially could disturb normal cellular membrane flux.

In summary, our data clearly show that the lysosomal cholesterol accumulation seen with ox-LDL is related in

some way to Golgi/TGN function. Although precise conclusions await further experiments, it is clear from our results that a better understanding of the relationship of lysosomal cholesterol accumulation and Golgi/TGN function will not only provide insight into two rare genetic disorders but will also have relevance to understanding atherogenesis.

The authors wish to thank Mr. Ken Grant, Ms. Stephanie Evans, and Ms. Paula Moore for technical assistance. This work was supported by NIH grant HL49148 (WGJ) and by grant 97F1005 from the American Heart Association, North Carolina Affiliate (PGY).

Manuscript received 15 October 1997 and in revised form 16 March 1998.

REFERENCES

1. Jerome, W. G., and J. C. Lewis. 1985. Early atherogenesis in White Carneau pigeons. II. Ultrastructural and cytochemical observations. *Am. J. Pathol.* **119:** 210–222.
2. Fowler, S., P. Berberian, H. Shio, S. Goldfischer, and H. Wolinsky. 1980. Characterization of cell populations isolated from aortas of rhesus monkeys with experimental atherosclerosis. *Circ. Res.* **46:** 520–530.
3. Miller, B., and H. Kothari. 1969. Increased activity of lysosomal enzymes in human atherosclerotic aortas. *Exp. Mol. Pathol.* **10:** 288–294.
4. Goldfischer, S., B. Schiller, and H. Wolinsky. 1975. Lipid accumulation in smooth muscle cell lysosomes in primate atherosclerosis. *Am. J. Pathol.* **78:** 497–504.
5. Jerome, W. G., and J. C. Lewis. 1997. Cellular dynamics in early atherosclerotic lesion progression in White Carneau pigeons. Spatial and temporal analysis of monocyte and smooth muscle invasion of the intima. *Arterioscler. Thromb. Vasc. Biol.* **17:** 654–664.
6. Gaton, E., D. Ben-Yshai, and M. Wolman. 1976. Experimentally produced hypertension and aortic acid esterase. *Arch. Pathol. Lab. Med.* **100:** 527–530.
7. Jerome, W. G., and J. C. Lewis. 1990. Early atherogenesis in White Carneau pigeons. Effect of a short-term regression diet. *Exp. Mol. Pathol.* **53:** 223–238.
8. Fogelman, A. M., M. E. Haberland, J. Seager, M. Hokom, and P. Edwards. 1981. Factors regulating the activities of low density lipoprotein receptor and the scavenger receptor on human monocyte-macrophages. *J. Lipid Res.* **22:** 1131–1141.
9. Goldstein, J. L., Y. K. Ho, S. K. Basu, and M. S. Brown. 1979. Binding sites on macrophages that mediate uptake and degradation of acetylated low density lipoprotein, producing massive cholesterol deposition. *Proc. Natl. Acad. Sci. USA.* **76:** 333–337.
10. Brown, M. S., and J. L. Goldstein. 1986. A receptor-mediated pathway for cholesterol homeostasis. *Science.* **232:** 34–47.
11. Mahley, R. W., T. L. Innerarity, K. H. Weisgraber, and S. Y. Oh. 1979. Altered metabolism (in vivo and in vitro) of plasma lipoproteins after selective chemical modification of lysine residues of the apoproteins. *J. Clin. Invest.* **64:** 743–750.
12. Adelman, S. J., and R. W. St Clair. 1988. Lipoprotein metabolism by macrophages from atherosclerosis-susceptible White Carneau pigeons and resistant Show Racer pigeons. *J. Lipid Res.* **29:** 643–656.
13. Tabas, I., S. Lim, X. X. Xu, and F. R. Maxfield. 1990. Endocytosed β-VLDL and LDL are delivered to different intracellular vesicles in mouse peritoneal macrophages. *J. Cell Biol.* **111:** 929–940.
14. Tabas, I., J. Myers, T. Innerarity, X. Xu, J. Arnold, and F. Maxfield. 1991. The influence of particle size and multiple apoprotein E-receptor interactions on the endocytic targeting of β-VLDL in mouse. *J. Cell Biol.* **115:** 1547–1560.
15. Steinberg, D., S. Parthasarathy, T. Carew, J. Khoo, and J. Witztum. 1989. Beyond cholesterol, modification of low-density lipoproteins that increase its atherogenicity. *N. Engl. J. Med.* **320:** 915–924.
16. Roma, P., A. Catapano, S. M. Bertulli, L. Varesi, R. Fumagalli, and F. Bernini. 1990. Oxidized LDL increase free cholesterol and fail to stimulate cholesterol esterification in murine macrophages. *Biochem. Biophys. Res. Commun.* **171:** 123–131.
17. Aviram, M. 1993. Modified forms of low density lipoprotein and atherosclerosis. *Atherosclerosis.* **98:** 1–9.
18. Barakat, H. A., and R. W. St. Clair. 1985. Characterization of plasma lipoproteins of grain- and cholesterol-fed White Carneau and Show Racer pigeons. *J. Lipid Res.* **26:** 1252–1268.
19. Basu, S. K., J. L. Goldstein, R. Anderson, and M. S. Brown. 1976. Degradation of cationized low density lipoprotein and regulation of cholesterol metabolism in homozygous hypercholesterolemia fibroblasts. *Proc. Natl. Acad. Sci. USA.* **73:** 3178–3182.
20. Buege, J., and S. Aust. 1978. Microsomal lipid peroxidation. *Methods Enzymol.* **52:** 302–310.
21. Lowry, O. H., N. J. Rosebrough, A. L. Farr, and R. J. Randall. 1951. Protein measurement with the Folin phenol reagent. *J. Biol. Chem.* **193:** 265–275.
22. Yancey, P. G., and R. W. St. Clair. 1992. Cholesterol efflux is defective in macrophages from atherosclerosis-susceptible White Carneau pigeons relative to resistant Show Racer pigeons. *Arterioscler. Thromb.* **12:** 1291–1304.
23. Denholm, E., and J. C. Lewis. 1987. Monocyte chemoattractants in pigeon aortic atherosclerosis. *Am. J. Pathol.* **126:** 464–475.
24. Bernard, D., A. Rodriques, G. Rothblast, and J. Glick. 1990. Influence of high density lipoprotein on esterified cholesterol stores in macrophages and hepatoma cells. *Arteriosclerosis.* **10:** 135–144.
25. Ishikawa, T. T., J. MacGee, J. A. Morrison, and C. J. Glueck. 1974. Quantitative analysis of cholesterol in 5 to 20 μl of plasma. *J. Lipid Res.* **15:** 286–291.
26. Gomori, G. 1950. An improved histochemical technic for acid phosphatase. *Stain Technol.* **25:** 81–85.
27. Weibel, E. R. 1969. Stereologic principles for morphometry in electron microscopic cytology. *Int. Rev. Cytol.* **26:** 235–302.
28. Webber, R. 1994. Self-calibrated tomosynthetic radiographic-imaging system, method, and device. , United States Patent #5,359,637.
29. Webber, R., R. Horton, D. Tyndall, and J. Ludlow. 1997. Tuned-aperture computed tomography (TACT). Theory and application for three-dimensional dentoalveolar imaging. *Dentomaxillifacial Radiol.* **26:** 53–62.
30. Lougheed, M., H. Zhang, and U. Steinbrecher. 1991. Oxidized low density lipoprotein is resistant to cathepsins and accumulates within macrophages. *J. Biol. Chem.* **266:** 14519–14525.
31. Jialal, I., and A. Chait. 1989. Differences in the metabolism of oxidatively modified low density lipoproteins and acetylated low density lipoprotein by human endothelial cells: inhibition of cholesterol esterification by oxidatively modified low density lipoprotein. *J. Lipid Res.* **30:** 1561–1568.
32. Roma, P., F. Bernini, R. Fogliatto, S. M. Bertulli, S. Negri, R. Fumagalli, and A. L. Catapano. 1992. Defective catabolism of oxidized LDL by J774 murine macrophages. *J. Lipid Res.* **33:** 819–829.
33. Maor, I., and M. Aviram. 1994. Oxidized low density lipoprotein leads to macrophage accumulation of unesterified cholesterol as a result of lysosomal trapping of the lipoprotein hydrolyzed cholesteryl ester. *J. Lipid Res.* **35:** 803–819.
34. Steinberg, D. 1996. Oxidized low density lipoprotein—an extreme example of lipoprotein heterogeneity. *Isr. J. Med. Sci.* **32:** 469–472.
35. Carpenter, K., G. Wilkins, B. Fussell, J. Ballantine, S. Taylor, M. Mitchnison, and D. Leake. 1994. Production of oxidized lipids during modification of low-density lipoprotein by macrophages or copper. *Biochem. J.* **304:** 625–633.
36. Brown, A., R. Dean, and W. Jessup. 1996. Free and esterified oxysterol: formation during copper-oxidation of low density lipoprotein and uptake by macrophages. *J. Lipid Res.* **37:** 320–335.
37. Greenspan, P., H. Yu, F. Mao, and R. Gutman. 1997. Cholesterol deposition in macrophages: foam cell formation mediated by cholesterol-enriched oxidized low density lipoprotein. *J. Lipid Res.* **38:** 101–109.
38. Yancey, P. G., and W. G. Jerome. 1998. Lysosomal sequestration of free and esterified cholesterol from oxidized low density lipoprotein in macrophages of different species. *J. Lipid Res.* **39:** 1349–1361.
39. Brown, M. S., and J. L. Goldstein. 1983. Lipoprotein metabolism in the macrophage. *Annu. Rev. Biochem.* **52:** 223–261.
40. Sparrow, C., S. Parthasarathy, and D. Steinberg. 1989. A macrophage receptor that recognizes oxidized low density lipoprotein but not acetylated low density lipoprotein. *J. Biol Chem.* **264:** 2599–2604.
41. Steinbrecher, U., M. Lougheed, W. Kwan, and M. Dirks. 1989. Recognition of oxidized low density lipoprotein by the scavenger receptor of macrophages results from derivatization of apolipopro-

tein B by products of fatty acid peroxidation. *J. Biol. Chem.* **264:** 15216–15223.
42. Maor, I., H. Mandel, and M. Aviram. 1995. Macrophage uptake of oxidized LDL inhibits lysosomal sphingomyelinase, thus causing the accumulation of unesterified cholesterol–sphingomyelin-rich particles in the lysosomes: a possible role for 7-ketocholesterol. *Arterioscler. Thromb. Vasc. Biol.* **15:** 1378–1387.
43. Jerome, W. G., L. K. Minor, J. M. Glick, G. H. Rothblat, and J. C. Lewis. 1991. Lysosomal lipid accumulation in vascular smooth muscle cells. *Exp. Mol. Pathol.* **54:** 144–158.
44. Pelham, H., and S. Munro. 1993. Sorting of membrane proteins in the secretory pathway. *Cell.* **75:** 603–605.
45. Griffiths, G. 1989. The structure and function of a mannose 6-phosphate receptor-enriched, pre-lysosomal compartment in animal cells. *J. Cell Sci*. **Suppl. 11:** 139–147.
46. Klausner, R., J. Donaldson, and J. Lippincott-Schwartz. 1992. Brefeldin A: insights into the control of membrane traffic and organelle structure. *J. Cell Biol.* **116:** 1071–1080.
47. Cooper, M. S., A. H. Cornell-Bell, A. Chernjavsky, J. W. Dani, and S. J. Smith. 1990. Tubulovesicular processes emerge from trans-Golgi cisternae, extend along microtubules, and interlink adjacent trans-Golgi elements into a reticulum. *Cell.* **61:** 135–145.
48. Weidman, P., R. Roth, and J. Heuser. 1993. Golgi membrane dynamics imaged by freeze-etch electron microscopy: views of different membrane coatings involved in tubulation versus vesiculation. *Cell*. **75:** 123–133.
49. Donaldson, J., R. Kahn, J. Lippincott-Schwartz, and R. Klausner. 1991. Binding of ARF and β-COP to Golgi membranes, possible regulation by a trimeric G protein. *Science.* **254:** 1197–1199.
50. Cluett, E., S. Wood, M. Banta, and W. Brown. 1993. Tubulation of Golgi membranes in vivo and in vitro in the absence of brefeldin A. *J. Cell Biol.* **120:** 15–24.
51. Griffiths, G., S. Fuller, R. Back, M. Hollinshead, S. Pfeiffer, and K. Simons. 1989. The dynamic nature of the Golgi complex. *J. Cell Biol*. **108:** 277–297.
52. Liscum, L., and K. Underwood. 1995. Intracellular cholesterol transport and compartmentation. *J. Biol. Chem.* **270:** 15443–15446.
53. Jourd'heuil, D., P. Vaananen, and J. Meddings. 1993. Lipid peroxidation of the brush-border membrane: membrane physical properties and glucose transport. *Am. J. Physiol*. **246:** 1009–1015.
54. Hannan, L. A., and M. Edidin. 1996. Traffic, polarity, and detergent solubility of a glycosylphosphatidylinositol-anchored protein after LDL-deprivation of MDCK cells. *J. Cell Biol*. **133:** 1265–1276.
55. Miccheli, A., A. Tomassini, R. Ricciolini, M. E. Di Cocco, E. Piccolella, C. Manetti, and F. Conti. 1994. Dexamethasone-dependent modulation of cholesterol levels in human lymphoblastoid B cell line through sphingosine production. *Biochim. Biophys. Acta*. **1221:** 171–177.
56. Zucker, S. D., W. Goessling, M. L. Zeidel, and J. L. Gollan. 1994. Membrane lipid composition and vesicle size modulate bilirubin intermembrane transfer. Evidence for membrane-directed trafficking of bilirubin in the hepatocyte. *J. Biol. Chem.* **269:** 19262–19270.
57. Robenek, H., and G. Schmitz. 1991. Abnormal processing of Golgi elements and lysosomes in Tangier disease. *Arterioscler. Thromb*. **11:** 1007–1020.
58. Coxey, R. A., P. G. Pentchev, G. Campbell, and E. J. Blanchette-Mackie. 1993. Differential accumulation of cholesterol in Golgi compartments of normal and Niemann-Pick type C fibroblasts incubated with LDL: a cytochemical freeze-fracture study. *J. Lipid Res.* **34:** 1165–1176.
59. Tabas, I., S. Marathe, G. Keesler, N. Beatini, and Y. Shiratori. 1996. Evidence that the initial up-regulation of phosphatidyl biosynthesis in free cholesterol-loaded macrophages is an adaptive response that prevents cholesterol-induced cellular necrosis. Proposed role of an eventual failure of this response in foam cell necrosis in advanced atherosclerosis. *J. Biol. Chem.* **271:** 22773–22781.